Proceedings of ASME Turbo Expo 2011
GT2011
June 6-10, 2011, Vancouver, British Columbia, Canada

GT2011-45309

THE INFLUENCE OF CRYSTAL ORIENTATION ON THE ELASTIC STRESSES OF A SINGLE CRYSTAL NICKEL-BASED TURBINE BLADE

Michael W. R. Savage
Siemens Industrial Turbomachinery Ltd
Lincoln, England

ABSTRACT

Single crystal nickel-based turbine blades are directionally solidified during the casting process with the crystallographic direction [001] aligned with the blade stacking axis. This alignment is usually controlled within 10°, known as the Primary angle. The rotation of the single crystal about the [001] axis is generally not controlled and this is known as the Secondary angle. The variation in Primary and Secondary angles relative to the blade geometry means that the stress response from blade to blade will be different, even for the same loading conditions. This paper investigates the influence of single crystal orientation on the elastic stresses of a CMSX-4 turbine blade root attachment using finite element analysis. The results demonstrate an appreciable variation in elastic stress when analysed over the controlled Primary angle, and are further compounded by the uncontrolled Secondary angle. The maximum stress range will have a direct impact on the fatigue resistance of the turbine blade. By optimizing the Secondary angle variation the elastic stresses can be reduced, giving the potential to enhance the fatigue resistance of the turbine blade.

INTRODUCTION

Single crystal nickel-based materials, such as CMSX-4 are commonly used for turbine blade applications due to their superior creep and fatigue properties at high temperature. The crystal structure of these materials is face-centered cubic (FCC), and due to their cubic symmetry have the same elastic constants in the principal crystallographic directions [100], [010] and [001]. However, in other crystallographic directions, for example [111], the elastic constants will change. As the elastic constants are sensitive to direction, variation in single crystal orientation relative to the blade geometry will directly affect the turbine blade elastic stresses and hence durability. If any one of the principal crystallographic directions is aligned in the direction of maximum radial stress caused by the centrifugal loading, then this will offer the best performance with respect to creep and fatigue.

During the casting process the turbine blade is directionally solidified so that the crystallographic direction [001] aligns with the blade stacking axis. Due to casting variability, a perfect alignment of the [001] axis or Primary axis is not practical. The Primary axis is usually controlled within an imaginary cone spanning up to 10° of the stacking axis, known as the Primary angle, α. The rotation of the single crystal about the Primary axis is known as the Secondary angle, β, which is generally not controlled, see Figure 1.

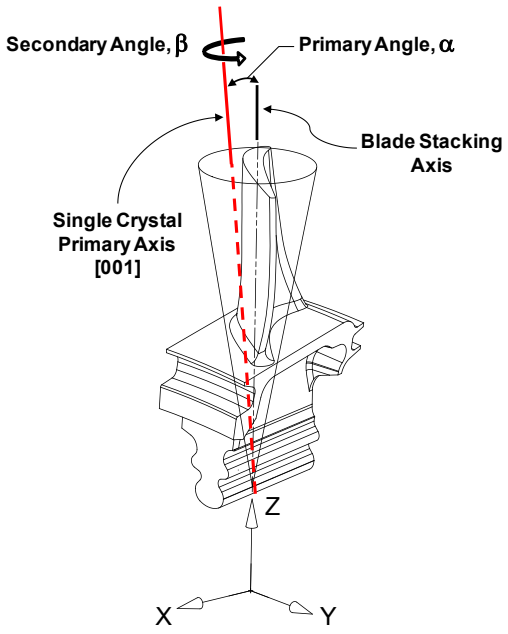

Figure 1. A turbine blade showing the Primary axis located within the limits defined by an imaginary cone.

Copyright © 2011 by ASME

COORDINATE TRANSFORMATION OF STRESS AND STRAIN

The state of stress at a point is defined by a stress tensor, consisting of 9 stress components of which 6 are independent (i.e. 3 normal stresses and 3 shear stresses). The stress tensor components are usually defined in a Cartesian coordinate system and expressed in a 3 x 3 matrix [1].

$$[\sigma]=\begin{bmatrix}\sigma_{11} & \sigma_{12} & \sigma_{13}\\ \sigma_{21} & \sigma_{22} & \sigma_{23}\\ \sigma_{31} & \sigma_{32} & \sigma_{33}\end{bmatrix}=\begin{bmatrix}\sigma_x & \tau_{xy} & \tau_{xz}\\ \tau_{yx} & \sigma_y & \tau_{yz}\\ \tau_{zx} & \tau_{zy} & \sigma_z\end{bmatrix} \quad (1)$$

Stress is a 2nd rank tensor (i.e. it requires magnitude and two directions). Using coordinate transformation laws, a stress tensor at a point can be expressed in a different Cartesian coordinate system [2]. For example, a stress tensor can be expressed in the turbine blade coordinate system (X, Y, Z) or in the material (single crystal) coordinate system (X^m, Y^m, Z^m) and vice versa. Using a 3 x 3 matrix, the transformation is given by,

$$[\sigma']=[A][\sigma][A]^T \quad (2)$$

where $[\sigma']$ is the stress tensor in the rotated coordinate system indicated by the prime, and $[A]$ is called the transformation (or rotation) matrix, and contains the direction cosines between the two coordinate systems.

$$[A]=\begin{bmatrix}A_{11} & A_{12} & A_{13}\\ A_{21} & A_{22} & A_{23}\\ A_{31} & A_{32} & A_{33}\end{bmatrix} \quad (3)$$

It is often more convenient to define the elements of the transformation matrix using Eulerian angles. This method can involve up to 3 successive rotations about an orthogonal axis in order to define the required orientation, as illustrated in Figure 2. The first rotation is by angle ϕ about the Z axis.

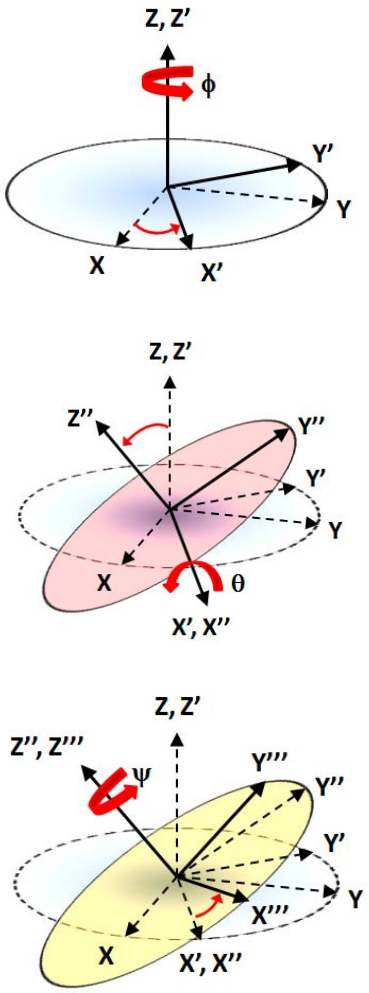

Figure 2. Eulerian angles involving three rotations.

The second rotation is by angle θ about the X' axis. The third rotation is by angle ψ about the Z'' axis. With regard to single crystal orientation, the first and second rotations define the Primary axis (with the second rotation known as the Primary angle). The third rotation defines the Secondary angle about the Primary axis. The transformation matrix for each rotation is given below and can be multiplied together to form the elements of the transformation matrix $[A]$. Eulerian angles will be used throughout this paper to define crystal orientation.

$$[A_z]=\begin{bmatrix}\cos\phi & \sin\phi & 0\\ -\sin\phi & \cos\phi & 0\\ 0 & 0 & 1\end{bmatrix} \quad (4)$$

Copyright © 2011 by ASME

$$[A_{x'}] = \begin{bmatrix} 1 & 0 & 0 \\ 0 & \cos\theta & \sin\theta \\ 0 & -\sin\theta & \cos\theta \end{bmatrix} \quad (5)$$

$$[A_{z''}] = \begin{bmatrix} \cos\psi & \sin\psi & 0 \\ -\sin\psi & \cos\psi & 0 \\ 0 & 0 & 1 \end{bmatrix} \quad (6)$$

$$[A] = [A_{z''}][A_{x'}][A_z] \quad (7)$$

Strain is also a 2nd rank tensor and can be expressed in a different Cartesian coordinate system using the same methods as described above for stress. The off diagonal strain tensor terms are known as the shear strains and equal to one-half of the engineering shear strain.

$$[\varepsilon] = \begin{bmatrix} \varepsilon_{11} & \varepsilon_{12} & \varepsilon_{13} \\ \varepsilon_{21} & \varepsilon_{22} & \varepsilon_{23} \\ \varepsilon_{31} & \varepsilon_{32} & \varepsilon_{33} \end{bmatrix} = \begin{bmatrix} \varepsilon_x & \varepsilon_{xy} & \varepsilon_{xz} \\ \varepsilon_{yx} & \varepsilon_y & \varepsilon_{yz} \\ \varepsilon_{zx} & \varepsilon_{zy} & \varepsilon_z \end{bmatrix} \quad (8)$$

Transformation law for strain;

$$[\varepsilon'] = [A][\varepsilon][A]^T \quad (9)$$

Up to this point coordinate transformation of stress and strain tensors have been described using 3 x 3 matrices. The same transformation can be achieved when the stress and strain tensors are expressed as 6 x 1 column vectors [2]. This approach is required for the stress-strain relationship as will be shown in the following section. In column vector form, the stress tensor can be transformed using,

$$\{\sigma'\} = [\underline{A}]\{\sigma\} \quad (10)$$

where $[\underline{A}]$ is a 6 x 6 transformation matrix. The first column vector of $[\underline{A}]$ is defined by using (2) and setting $\sigma_{11} = 1$ in the stress tensor (all other stress components are set to zero). The resulting 3 x 3 matrix is then unfolded giving the first column vector. This process is repeated for all stress components using the same sequence as defined by the stress column vector. In the case of shear stresses, $\sigma_{ij} = \sigma_{ji} = 1$ is set for the stress tensor. Completing this process $[\underline{A}]$ is defined as,

$$[\underline{A}] = \begin{bmatrix} A_{11}A_{11} & A_{12}A_{12} & A_{13}A_{13} & 2A_{12}A_{13} & 2A_{11}A_{13} & 2A_{11}A_{12} \\ A_{21}A_{21} & A_{22}A_{22} & A_{23}A_{23} & 2A_{22}A_{23} & 2A_{21}A_{23} & 2A_{21}A_{22} \\ A_{31}A_{31} & A_{32}A_{32} & A_{33}A_{33} & 2A_{32}A_{33} & 2A_{31}A_{33} & 2A_{31}A_{32} \\ A_{21}A_{31} & A_{22}A_{32} & A_{23}A_{33} & A_{22}A_{33} + A_{23}A_{32} & A_{21}A_{33} + A_{23}A_{31} & A_{21}A_{32} + A_{22}A_{31} \\ A_{11}A_{31} & A_{12}A_{32} & A_{13}A_{33} & A_{12}A_{33} + A_{13}A_{32} & A_{11}A_{33} + A_{13}A_{31} & A_{11}A_{32} + A_{12}A_{31} \\ A_{11}A_{21} & A_{12}A_{22} & A_{13}A_{23} & A_{12}A_{23} + A_{13}A_{22} & A_{11}A_{23} + A_{13}A_{21} & A_{11}A_{22} + A_{12}A_{21} \end{bmatrix} \quad (11)$$

Copyright © 2011 by ASME

Similarly, the strain tensor in column vector form can be transformed using,

$$\{\varepsilon'\} = [\underline{A}]\{\varepsilon\} \tag{12}$$

It is often required to express the shear strain tensor as engineering shear strain. This can be achieved using,

$$\{\varepsilon_{eng}\} = [R]\{\varepsilon\} \tag{13}$$

where $\{\varepsilon_{eng}\}$ signifies engineering shear strain, and $[R]$ is called the Reuter matrix [3] defined as,

$$[R] = \begin{bmatrix} 1 & 0 & 0 & 0 & 0 & 0 \\ 0 & 1 & 0 & 0 & 0 & 0 \\ 0 & 0 & 1 & 0 & 0 & 0 \\ 0 & 0 & 0 & 2 & 0 & 0 \\ 0 & 0 & 0 & 0 & 2 & 0 \\ 0 & 0 & 0 & 0 & 0 & 2 \end{bmatrix} \tag{14}$$

ELASTIC STRESS-STRAIN RESPONSE OF CUBIC MATERIALS

If a material deforms linear-elastically it can be represented by Hooke's law. This means that the 6 stress components are linearly related to the 6 strain components. In matrix form Hooke's law may be generalised as,

$$\{\varepsilon_{eng}\} = [S]\{\sigma\} \tag{15}$$

$$\{\sigma\} = [C]\{\varepsilon_{eng}\} \tag{16}$$

where $[S]$ is the compliance matrix and $[C]$ is the stiffness matrix. Both these quantities represent 4th rank tensors, but can be reduced to 6 x 6 matrices due to symmetry in stress and strain. The stress tensor and engineering strain are expressed as column vectors. The compliance matrix for a cubic material in the principal crystallographic directions [100], [010] and [001] is defined below. For this condition the elements of the compliance matrix are related by $S_{11} = S_{22} = S_{33}$, $S_{12} = S_{13} = S_{23}$ and $S_{44} = S_{55} = S_{66}$. A cubic material has 3 elastic constants: Young's modulus E, the modulus of rigidity G, and Poisson's ratio ν. For isotropic materials it is customary to define G in terms of E and ν. This is not valid for cubic materials as the 3 elastic constants are independent.

$$[S] = \begin{bmatrix} \frac{1}{E} & \frac{-\nu}{E} & \frac{-\nu}{E} & 0 & 0 & 0 \\ \frac{-\nu}{E} & \frac{1}{E} & \frac{-\nu}{E} & 0 & 0 & 0 \\ \frac{-\nu}{E} & \frac{-\nu}{E} & \frac{1}{E} & 0 & 0 & 0 \\ 0 & 0 & 0 & \frac{1}{G} & 0 & 0 \\ 0 & 0 & 0 & 0 & \frac{1}{G} & 0 \\ 0 & 0 & 0 & 0 & 0 & \frac{1}{G} \end{bmatrix} \tag{17}$$

In other crystallographic directions (or loading directions), the elastic constants will change [3]. The extreme values of E in a cubic material occur in the [100] and [111] directions and when expressed as a ratio $E_{[111]}/E_{[100]}$ this provides a measure of anisotropy. For nickel the ratio is ~2.3 and can be calculated from the elastic compliances [4] as defined below.

$$\frac{E_{[111]}}{E_{[100]}} = \frac{3S_{11}}{(S_{11} + 2S_{12} + S_{44})} \tag{18}$$

When the loading is not in the principal crystallographic directions the compliance matrix needs to be evaluated. As an example, consider a plain specimen under load-controlled conditions. The applied load and hence stress tensor will be known in the specimen axial direction. Using either (2) or (10) with knowledge of the single crystal orientation relative to the specimen, the stress tensor can be calculated in the principal crystallographic directions. Also, the corresponding engineering strain can be calculated using (15). To calculate the engineering strain in the specimen axial direction, a new compliance matrix must be formed to reflect the changes in elastic constants. Note that the transformation matrix $[A]$ used to find the stress tensor in the principal crystallographic directions and the engineering strain in the specimen axial direction will be different due to the sense of the angles.

The engineering strain in the specimen axial direction $\{\varepsilon'_{eng}\}$ can be calculated by deriving (15) for a rotated coordinate system.

$$\{\varepsilon'_{eng}\} = [R]\{\varepsilon'\} = [R][\underline{A}]\{\varepsilon\} = [R][\underline{A}][R]^{-1}\{\varepsilon_{eng}\}$$

$$\{\varepsilon'_{eng}\} = [R][\underline{A}][R]^{-1}[S]\{\sigma\} = [R][\underline{A}][R]^{-1}[S][\underline{A}]^{-1}\{\sigma'\}$$

Copyright © 2011 by ASME

$$\{\varepsilon'_{eng}\} = [S']\{\sigma'\} \tag{19}$$

where $[S'] = [R][\underline{A}][R]^{-1}[S][\underline{A}]^{-1}$ is the compliance matrix in the rotated coordinate system.

Let's assume a nickel single crystal specimen at room temperature is loaded in tension with a stress of 300 MPa in the axial direction as shown in Figure 3. Nickel is a cubic material and the elastic compliances in the principal crystallographic directions [100], [010] and [001] are typically, S_{11} = 0.769 x 10^{-5} /MPa, S_{12} = -0.292 x 10^{-5} /MPa and S_{44} = 0.836 x 10^{-5} /MPa [5]. In these principal directions the elastic constants are the same and can be calculated by equating the elastic compliances to the elements in (17) giving, E = 130039 MPa, G = 119617 MPa, and ν = 0.38.

Using the definitions given above the Eulerian angles for the single crystal orientation are given by ϕ = 0°, θ = 10° and ψ = 0° (this is equivalent to a Primary angle of 10° and a Secondary angle of 0°).

The angles defining the single crystal orientation are used with matrices (4-6) and combined using (7) to form the 3 x 3 transformation matrix $[A]$ giving,

$$[A] = \begin{bmatrix} 1 & 0 & 0 \\ 0 & 0.985 & 0.174 \\ 0 & -0.174 & 0.985 \end{bmatrix}$$

The elements of this matrix are then substituted into (11) to form the 6 x 6 transformation matrix $[\underline{A}]$.

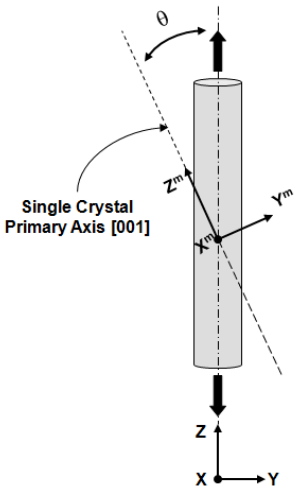

Figure 3. Test specimen showing the alignment of the single crystal Primary axis.

Using (10) the stress tensor in the principal crystallographic directions is,

$$\begin{Bmatrix} 0 \\ 9.05 \\ 290.95 \\ 51.30 \\ 0 \\ 0 \end{Bmatrix} = [\underline{A}] \begin{Bmatrix} 0 \\ 0 \\ 300 \\ 0 \\ 0 \\ 0 \end{Bmatrix}$$

and substituting the elastic constants into (17) and using (15), the engineering strain is,

$$\begin{Bmatrix} -0.000876 \\ -0.000780 \\ 0.002211 \\ 0.000429 \\ 0 \\ 0 \end{Bmatrix} = [S] \begin{Bmatrix} 0 \\ 9.05 \\ 290.95 \\ 51.30 \\ 0 \\ 0 \end{Bmatrix}$$

To calculate the engineering strain in the specimen axial direction, a new transformation matrix is required as the angle from the Primary axis to the specimen axial direction is in the opposite sense. Using the Eulerian angles ϕ = 0°, θ = -10° and ψ = 0°, the new 6 x 6 transformation matrix $[\underline{A}]$ is formed as previously described. The engineering strain in the specimen axial direction can be calculated using (19) where $[S']$ is the new compliance matrix in the rotated coordinate system. The engineering strain is,

$$\begin{Bmatrix} -0.000876 \\ -0.000763 \\ 0.002194 \\ -0.000620 \\ 0 \\ 0 \end{Bmatrix} = [S'] \begin{Bmatrix} 0 \\ 0 \\ 300 \\ 0 \\ 0 \\ 0 \end{Bmatrix}$$

TURBINE BLADE FINITE ELEMENT ANALYSIS

The influence of single crystal orientation on the elastic stresses of a CMSX-4 turbine blade root attachment using finite element analysis has been investigated. The approach taken and the results are summarised below.

Copyright © 2011 by ASME

A finite element model of the turbine blade and disc sector was created using PATRAN and solved using ABAQUS Standard. The finite element model is shown in Figure 4. The majority of the model was auto-meshed using quadratic tetrahedral elements. The blade and disc root pressure flanks were meshed separately and locally refined using linear hexahedral elements. The elements' density in these regions was increased significantly to capture the high stress gradients adjacent to the edge of contact and in the fillets. The tetrahedral and hexahedral dissimilar meshes were joined together using tied contact. At the blade and disc root interface, small sliding surface-to-surface contact was defined with friction.

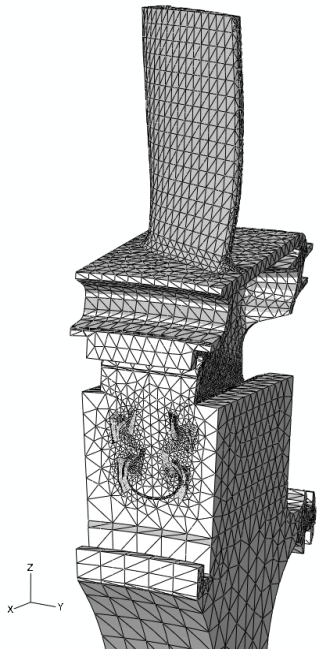

Figure 4. Finite element model of the turbine blade and disc sector.

Boundary conditions were added to the disc sector cut-boundary faces to represent cyclic symmetry. Rigid body motion of the disc is prevented by tangential and axial restraints applied to the upstream disc face, located at the hirth teeth. The blade was also constrained to the disc in the root axial direction to avoid rigid body motion. The finite element model was simulated under representative engine speed and temperature conditions.

The disc material is IN718, and modelled with isotropic behaviour. The single crystal turbine blade material is CMSX-4, and modelled with orthotropic behaviour. In ABAQUS, the orientation of the orthotropic material relative to the turbine blade is specified using the orientation keyword.

In order to quantify the effect of crystal orientation on the elastic stresses at the blade root, the simulation was repeated 81 times with different crystal orientations, see Table 1. The Eulerian angles are measured relative to the turbine blade coordinate system. The Secondary angle reference location $\psi = 0°$ is defined when the crystallographic direction [100] is in alignment with the X-axis of the turbine blade coordinate system.

Table 1. Simulated crystal orientations.

Primary Axis Location	Angle ϕ	Angle θ	Angle ψ
0	0	0	0, 10, 20, 30, 40, 50, 60, 70, 80
1	0	5	0
2	45	5	0
3	90	5	0
4	135	5	0
5	180	5	0
6	225	5	0
7	270	5	0
8	315	5	0
9	0	10	0, 10, 20, 30, 40, 50, 60, 70, 80
10	22.5	10	0
11	45	10	0, 15, 30, 45, 60, 75
12	67.5	10	0
13	90	10	0, 10, 20, 30, 40, 50, 60, 70, 80
14	135	10	0, 15, 30, 45, 60, 75
15	180	10	0, 10, 20, 30, 40, 50, 60, 70, 80
16	202.5	10	0
17	225	10	0, 15, 30, 45, 60, 75
18	247.5	10	0
19	270	10	0, 10, 20, 30, 40, 50, 60, 70, 80
20	315	10	0, 15, 30, 45, 60, 75

RESULTS AND DISCUSSION

The results of the above simulations were studied to investigate the influence of Primary and Secondary angle variation on the elastic stresses at the blade root attachment. The normalized Maximum Principal Stress distribution is shown in Figure 5 for a Primary and Secondary angle of 0°

Copyright © 2011 by ASME

(i.e. Location 0). The Primary axis locations are illustrated in Figure 6. At full load, the peak tensile stresses occur near to the edge of contact. The results being presented for discussion occur at the lower lobe suction side towards the trailing edge.

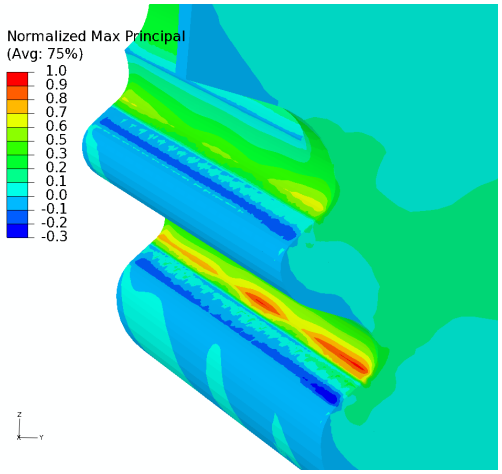

Figure 5. Normalized Maximum Principal Stress distribution of the blade root suction side.

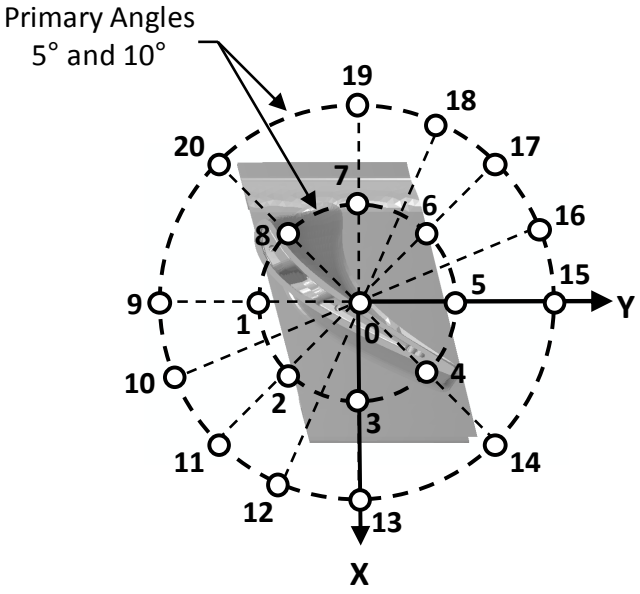

Figure 6. Plan view of the turbine blade illustrating the Primary axis locations at two Primary angles 5° and 10°.

The results in Figure 7 show how the Primary axis location defined by angles ϕ and θ, affects the normalized von Mises stress magnitude when Secondary angle $\psi = 0°$. For a given Primary angle, changing the Primary axis location causes the stress to fluctuate in a cyclic manner. For example, a Primary angle of $\theta = 10°$ has a 9.7% increase in stress compared to a perfectly aligned single crystal when the Primary axis is located by $\phi = 45°$. However, rotating the Primary axis to $\phi = 202.5°$, results in a stress reduction of 19%. The data points in Figure 7 are numbered in brackets and refer to the actual Primary axis location as illustrated in Figure 6. What is evident from the results is that when the Primary axis is leaning towards the stress being monitored (i.e. Lower lobe suction side towards trailing edge) the stress increases, whereas, when the Primary axis leans away from the stress being monitored the stress reduces. For a balanced blade root, whereby the stresses on the suction and pressure side are similar, no benefit would be obtained from the above observation, apart from reducing the Primary angle. To approximate the stress for other Primary angles (within the limits of $\theta = 0°$ to $\theta = 10°$) a response surface was created. The resulting contour plot is shown in Figure 8.

The results in Figure 9 show how the Secondary angle ψ affects the normalized von Mises stress magnitude. For a Primary angle $\theta = 0°$ the stress increases by 1% when $\psi = 15°$. For this Secondary angle the principal crystallographic direction [100] will be aligned along the blade root axial direction since the blade root has a skew angle of 15°. However, rotating the Secondary angle to $\psi = 60°$, results in a stress reduction of 5.6%. A contour plot illustrates this result, see Figure 10.

The Primary angle study found that the maximum stress occurred when the Primary angle $\theta = 10°$, and the Primary axis was located at $\phi = 45°$ (i.e. Location 11). Rotating the Secondary angle resulted in no increase in stress, but a reduction of 5.2% when $\psi = 50°$. However, this stress reduction would not be gained if the Primary axis was located at $\phi = 0°$ (i.e. Location 9). If the Secondary angle is nominally controlled in the region of $\psi = 56°$, then there is a potential to lower the maximum stress by 4% when $\theta = 10°$. A contour plot illustrates this result, see Figure 11. Choosing the required optimized Secondary angle needs to reflect all Primary axis locations, as their minimum stresses will not always coincide, as is evident from Figure 9. Also, it must be acknowledged that optimizing the Secondary angle at the blade root location may have an adverse effect at other blade locations, such as the aerofoil and therefore the whole blade must be considered.

Copyright © 2011 by ASME

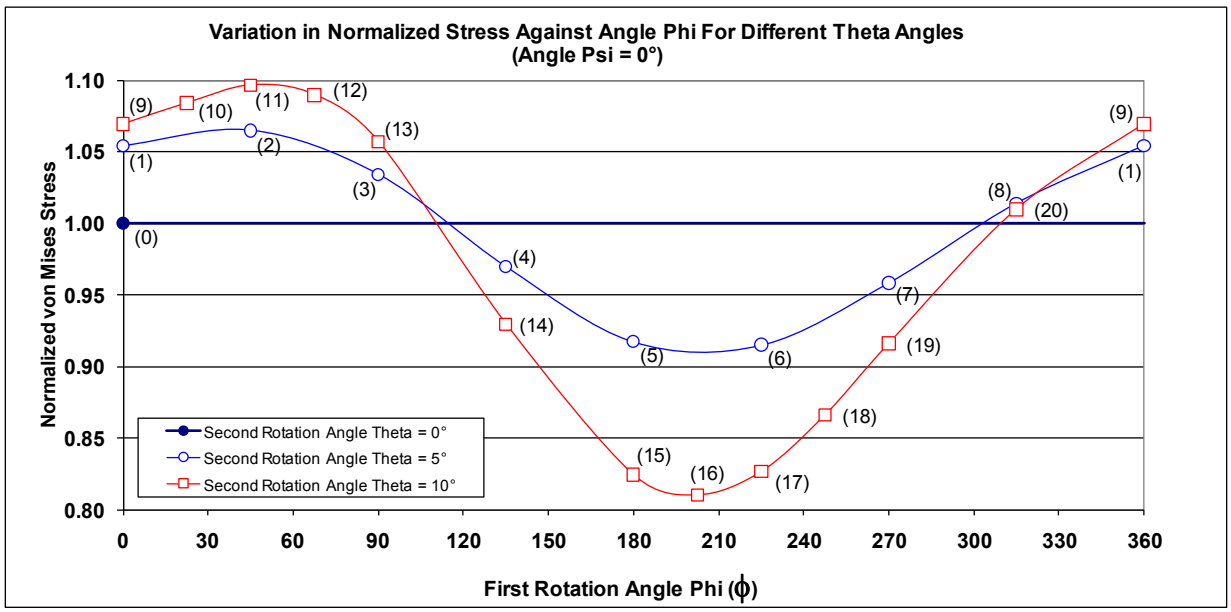

Figure 7. Variation in normalized von Mises stress against angle ϕ for Primary angles of 0°, 5° and 10° (Secondary angle is 0°).

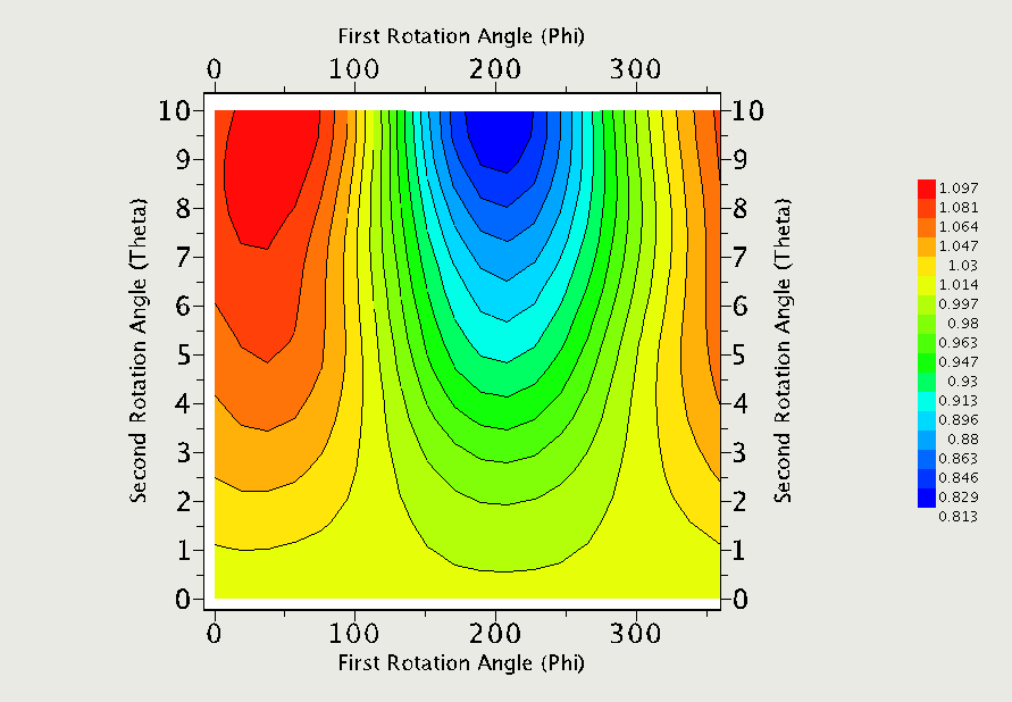

Figure 8. Contour plot showing the influence of the Primary angle and axis location on normalized von Mises stress.

Copyright © 2011 by ASME

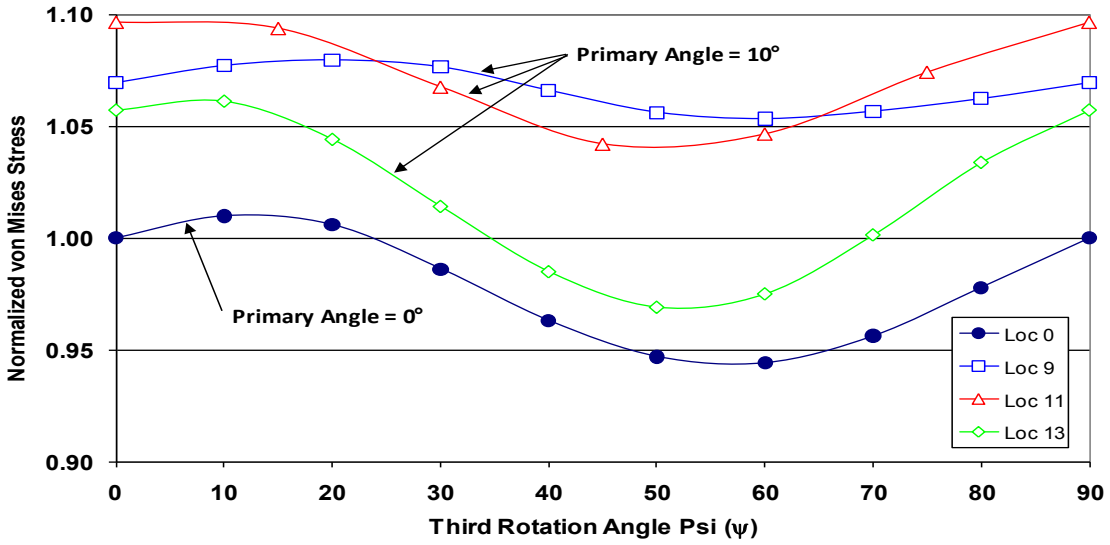

Figure 9. Variation in normalized von Mises stress against Secondary angle ψ for a Primary angle of 0° and 10°. Different Primary axis locations are shown for a Primary angle of 10°.

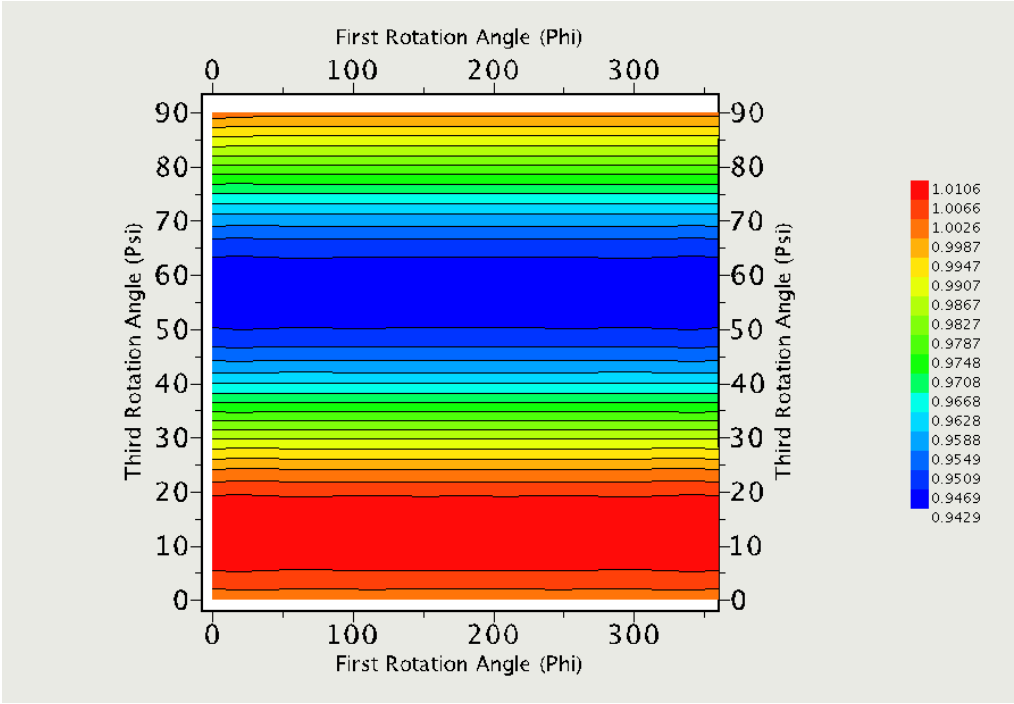

Figure 10. Contour plot showing the influence of the Secondary angle on normalized von Mises stress when the Primary angle is 0°.

Copyright © 2011 by ASME

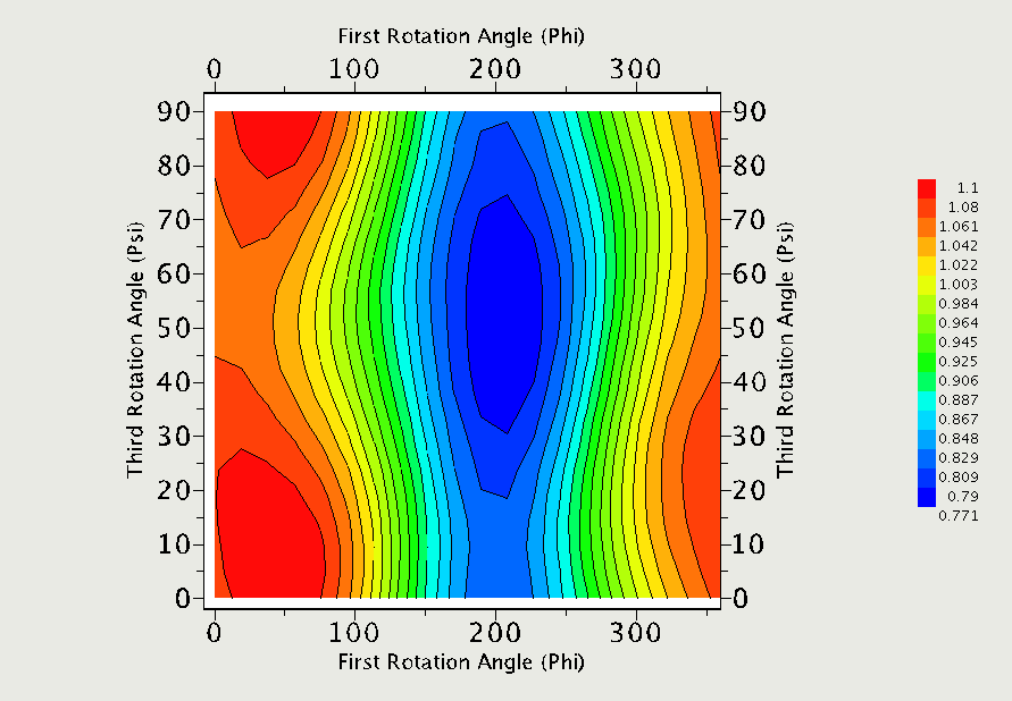

Figure 11. Contour plot showing the influence of the Secondary angle on normalized von Mises stress when the Primary angle is 10°.

CONCLUSION

Single crystal nickel-based materials, such as CMSX-4 have a FCC crystal structure, and due to their cubic symmetry have the same elastic constants in the principal crystallographic directions [100], [010] and [001]. The orientation of the single crystal relative to the component has a direct impact on the elastic state of stress, as the elastic constants change with direction.

The methodology for calculating the elastic state of stress given the single crystal orientation was explained and demonstrated using a simple specimen under load-control. The ability to determine the stresses (and strains) in the crystallographic directions is of interest when exploring suitable fatigue criteria involving slip planes [6].

The influence of single crystal orientation on the elastic stresses of a turbine blade root was not insignificant. For a Primary angle $\theta = 10^\circ$ the stress was found to fluctuate by +9.7% and -19% depending on the Primary axis location. If the Secondary angle is nominally controlled in the region of $\psi = 56^\circ$, then there is a potential to lower the maximum stress by 4% when $\theta = 10^\circ$ and to improve the fatigue resistance of the turbine blade root. Optimizing the Secondary angle at the blade root location may have an adverse effect at other blade locations, such as the aerofoil and therefore the whole blade must be considered.

These results indicate that care should be taken when using traditional deterministic approaches for fatigue life assessment as the results will only be valid for a given crystal orientation. An alternative approach would be to treat the crystal orientation as a random variable and use probabilistic methods.

REFERENCES

[1] Dieter, G. E., 1988, *Mechanical Metallurgy*, McGraw-Hill Book Co., Singapore.

[2] Slawinski, M. A., 2009, *Waves and Rays in Elastic Continua*, World Scientific Publishing Co, Singapore.

[3] Stouffer, D. C., and Dame, L. T., 1996, *Inelastic Deformation of Metals, Models, Mechanical Properties, and Metallurgy,* John Wiley & Son, Inc., New York.

[4] Hosford, W. F., 2005, *Mechanical Behavior of Materials,* Cambridge University Press, Cambridge.

[5] Smithells, C. J., 1967, *Metals Reference Book Vol. 3 (Fourth Edition)*, Butterworths, London.

[6] Arakere, N. K., and Swanson, G., 2002, "Effect of Crystal Orientation on Fatigue Failure of Single Crystal Nickel Base Turbine Blade Superalloys" Journal of Eng. For Gas Turbines and Power, **124**, pp. 161-175.

Copyright © 2011 by ASME